Transition to Oscillatory Convective Heat Transfer in a Fluid-Saturated Porous Medium

Cyrus K. Aidun* and Paul H. Steen†
Cornell University, Ithaca, New York

The transition from steady to time-periodic motion in the analog of Benard convection in a two-dimensional region of fluid-saturated porous media is studied by means of an eigenfunction expansion and a branch-tracing technique. This method leads to the location of the transition at Rayleigh number 9.9 times that at convection onset. The small-amplitude motion has a period 0.012 times shorter than the thermal diffusion time and comes into existence through a Hopf bifurcation. The structure and time progression of the destabilizing disturbance indicates that the dominant effect is an instability convected by the base flow whose strength is coupled to the steepening thermal boundary layers. The effects of truncation of the expansion on the prediction of the transition and its mechanism are discussed.

Nomenclature

a_i = amplitude function
C_{pf} = heat capacity of the fluid
C_{pm} = heat capacity of the fluid/solid mixture
g = acceleration of gravity
H = ratio of heat capacity per unit volume of fluid/solid mixture to that of the fluid
HB = Hopf bifurcation
I = maximum wave number in the truncation
j = unit vector opposite to the direction of gravity
k = permeability of the porous material
ℓ = dimension of the square
N = number of modes in the truncation
Nu = Nusselt number
n = unit normal vector
P = Prandtl number
p = pressure
R = Rayleigh number
R_c = critical Rayleigh number for convection onset
R_p = critical Rayleigh number for onset of periodic convection
ΔT = temperature difference between top and bottom of the box
TP = turning point
u = x component of macroscopic velocity
v = y component of macroscopic velocity
$\boldsymbol{v}$ = macroscopic velocity vector
X = vector of dependent variables
x = horizontal Cartesian coordinate
y = vertical Cartesian coordinate
β = coefficient of thermal expansion
Φ_i = eigenfunctions of the infinitesimal disturbances to the basic conduction state
κ_m = effective fluid/solid thermal diffusivity
υ = kinematic viscosity
ρ_f = density of the fluid
ρ_m = density of the fluid/solid mixture
Θ = disturbance in temperature relative to the basic conduction state
τ = dimensionless time
ψ = stream function

Received May 10, 1986; presented as Paper 86-1264 at the AIAA/ASME 4th Thermophysics and Heat Transfer Conference, Boston, MA, June 2-4, 1986; revision received Sept. 8, 1986.

*Postdoctoral Fellow, School of Chemical Engineering and Mathematical Sciences Institute. Member AIAA.
†Assistant Professor, School of Chemical Engineering and Mathematical Sciences Institute.

I. Introduction

THE heat transferred from bottom to top across a square container that is filled with fluid-saturated porous material and heated from below exhibits a sequence of transitions as the temperature difference across the box is increased. For temperature differences characterized by Rayleigh number R below a first critical value R_c, the fluid remains motionless and heat is transferred by pure conduction. For temperature gradients in a range above R_c, the buoyancy forces drive a steady convection. Beck[1] showed that $R_c = 4\pi^2$ by means of linear stability theory. As the Rayleigh number is increased further the steady motion is abruptly replaced by a time-periodic motion at $R = R_p$. Previous studies of this transition using conventional numerical techniques including finite-difference[2-4] and spectral methods[5] have reported estimates of R_p ranging from 280[4] to 380–400[5] over a period of years. Although a recent study[6] accurately predicts the frequency of motion at transition (in excellent agreement with our result) as well as the transition point, quantitative descriptions of the mechanism of instability are lacking. The slow decay of transients masks the periodic motion, and the nonlinear base state hides the small-amplitude disturbances. In contrast, the branch-tracing approach allows us to characterize the transition mechanism and solve for the structure of the unstable disturbances.

In addition to various applications,[7] the porous media system is a prototype of a class of hydrodynamic systems that exhibit a characteristic sequence of transitions from steady to time-periodic and eventually complicated time-dependent behavior.[8] A full understanding of the transition sequence for this particular hydrodynamic system can serve as a guide to the study of other technically important flows.

Two-dimensional convective motions have been observed experimentally,[9-11] yet the technical difficulty of direct measurements within porous media has prevented observations of the transition to time-periodicity that are sufficiently detailed to compare with quantitative predictions. Several studies do report "fluctuating" two-dimensional states.[12-14] There have been detailed observations, however, of a corresponding transition within the Hele Shaw Cell, an analog system, for geometries with aspect ratios of order one but not

square.[15,16] Although the different geometries prevent a quantitative comparison, there is a qualitative agreement.

II. Formulation

A square container is filled with a porous material and saturated with a viscous Boussinesq fluid. For pore structure small compared to the size of the box, a description in terms of a macroscopic velocity and Darcy's law is appropriate.[17] The dimensionless equations governing the arbitrary disturbances in velocity v, temperature Θ, and pressure p from the motionless state of pure conduction are given by

$$\mathbf{0} = R^{1/2}\Theta \boldsymbol{j} - \nabla p - \boldsymbol{v} \tag{1a}$$

$$\frac{\partial \Theta}{\partial \tau} + R^{1/2}\boldsymbol{v}\cdot(\nabla\Theta - \boldsymbol{j}) = \nabla^2\Theta \tag{1b}$$

$$\nabla\cdot\boldsymbol{v} = 0 \tag{1c}$$

The inertia term in the momentum equation (1a) is proportional to the permeability k of the porous material through a Prandtl number $P \equiv \nu\ell^2/\kappa_m k$ and is neglected since permeabilities are typically very small. The Rayleigh parameter $R \equiv g\beta\Delta T k\ell/\kappa_m\nu$ remains the only parameter in the equations (1). It characterizes the exchange of energy and momentum in the bulk. The product of the gravitational acceleration g, the coefficient of thermal expansion β, and the imposed temperature difference between top and bottom ΔT represents the buoyancy force per unit mass. Gravity acts antiparallel to the unit vector $\boldsymbol{j}$. A thermal diffusion time scale $\ell^2 H/\kappa_m$ is employed where $H \equiv \rho_m C_{pm}/\rho_f C_{pf}$ is the ratio of the heat capacity of the fluid/solid mixture to that of the fluid.

The boundary conditions are isothermal top and bottom, insulated sidewalls, and impermeable boundaries:

$$\Theta = 0 \qquad y = 0,1 \tag{2a}$$

$$\partial\Theta/\partial x = 0 \qquad x = \pm 1/2 \tag{2b}$$

$$\boldsymbol{v}\cdot\boldsymbol{n} = 0 \qquad \text{on all boundaries} \tag{2c}$$

Here $\boldsymbol{n}$ is the unit normal vector. We have used rectangular Cartesian coordinates with y increasing in a direction opposite to gravity and with the center of the box at (0, ½).

The key property of the system (1,2) is that the linear operator is self-adjoint; the sequence of associated eigenfunctions forms a complete set of orthogonal functions. Infinitesimal disturbances to the basic conduction state in the temperature, stream function, and pressure are given by

$$\Theta_i = \cos[(m\pi/2)(1+2x)]\ \sin n\pi y \tag{3a}$$

$$\psi_i = R^{1/2}(m\pi)\alpha_i\ \sin[(m\pi/2)(1+2x)]\ \sin n\pi y \tag{3b}$$

$$p_i = -R^{1/2}(n\pi)\alpha_i\ \cos[(m\pi/2)(1+2x)]\ \cos n\pi y \tag{3c}$$

where

$$\alpha_i = 1/[(m\pi)^2 + (n\pi)^2]$$

$$m = 0,1,2,\ldots;\ n = 1,2,\ldots;\ i = [m,n]$$

Here m and n are the wavenumbers in the x and y directions respectively; their combination characterizes the mode number i. The stream function is defined such that the x and y components of the velocity vector are given by

$$u = -\partial\psi/\partial y \text{ and } v = \partial\psi/\partial x$$

We expand the dependent variables in terms of the eigenfunctions of the linear problem

$$X(x,y,\tau;R) = \Sigma a_i(\tau)\Phi_i(x,y) \tag{4}$$

where $X \equiv [u, v, \Theta, p]$ and $\Phi_i \equiv [u_i, v_i, \Theta_i, p_i]$ are the vectors of dependent variables and eigenfunctions, respectively. Using the expansion equation (4), a Galerkin-like treatment yields an infinite number of ordinary differential equations in time for the amplitude functions a_i,

$$(C_i/R)\,da_i/d\tau = \lambda_i(1 - R_i/R)a_i + A_{ijk}a_j a_k \tag{5}$$

where $\lambda_i/C_i = 1 - n^2/(m^2+n^2)$, $C_i = 1 + \delta^o_m$, $R_i = \pi^2(m^2+n^2)/[1 - n^2/(m^2+n^2)]$, $i = 1,2\ldots$, and δ^o_m has a value of zero unless $m = 0$, in which case it has a value of one. The details of this derivation and the explicit form of the coefficient A_{ijk} are given elsewhere.[18]

III. Results and Discussion

System (5), with an infinite number of equations, is formally equivalent to the governing partial differential system (1,2). We truncate to N modes and treat the resulting finite-dimensional system as a bifurcation problem. This contrasts with previous spectral[5] and pseudospectral treatments[8] that view the finite system as an initial value problem. The conduction solution is stable (globally) up to $R_c = 4\pi^2$, where the first branch point occurs. An exchange of stability to a steady roll cell takes place here, characterized near the onset by eigen-

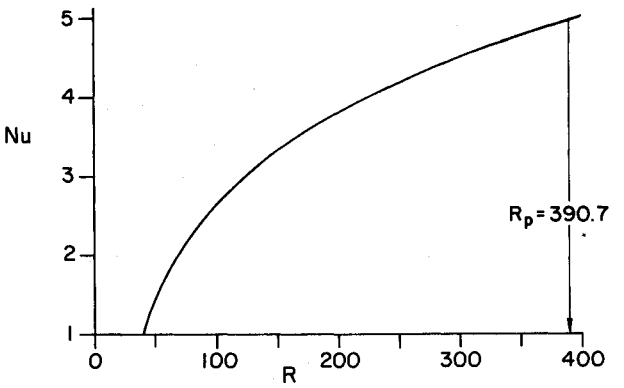

Fig. 1 Nusselt number Nu vs Rayleigh number R.

Table 1 Comparison of present results with finite-difference calculations

	Present results ($I = 18$)		Finite-difference[a] (48×48)	
R	Nu	Ψ_{max}	Nu	Ψ_{max}[b]
100	2.646	0.5378	2.651	0.5377
200	3.809	0.6326	3.813	0.6323
250	4.192	0.6485	4.199	0.6484
300	4.516	0.6583	4.523	0.6585

[a]From Ref. 3. [b]The maximum value of the stream function is rescaled by $R^{1/2}$.

Table 2 Effects of truncation on the predicted R_p

I	Predicted critical Rayleigh number	Type of bifurcation[a]
5	239.3	*HB*
6	256.2	*TP*
7	313.6	*HB*
8	304.4	*TP*
9	345.5	*HB*
10	348.4	*HB*
12	370.9	*HB*
14	385.9	*HB*
16	390.3	*HB*
17	390.7	*HB*
18	390.7	*HB*
30	390.7	*HB*

[a]*HB* = Hopf bifurcation, *TP* = turning point.

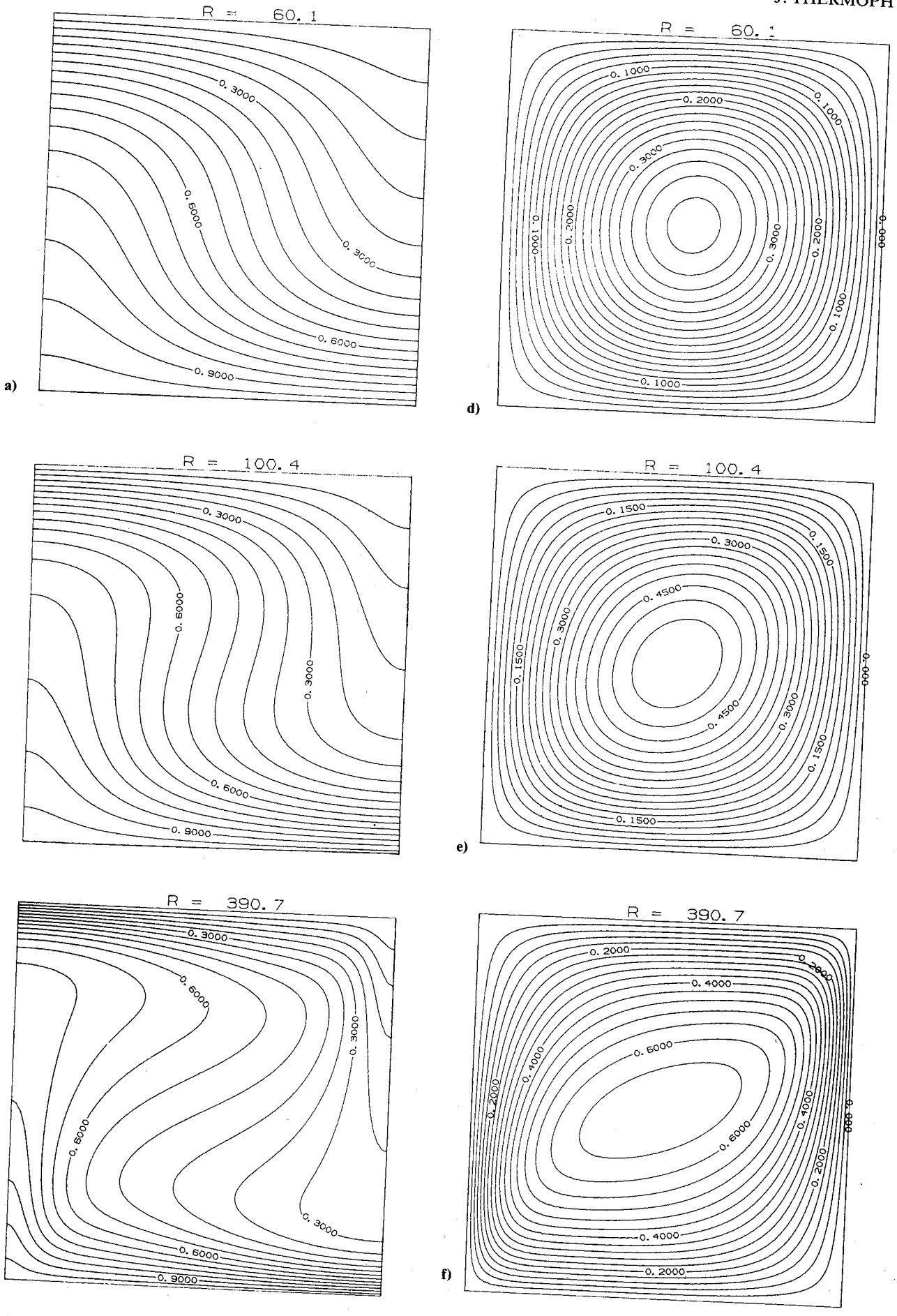

Fig. 2 Isotherms a)–c) and streamlines d)–f) corresponding to Rayleigh numbers, 60, 100, and 391.

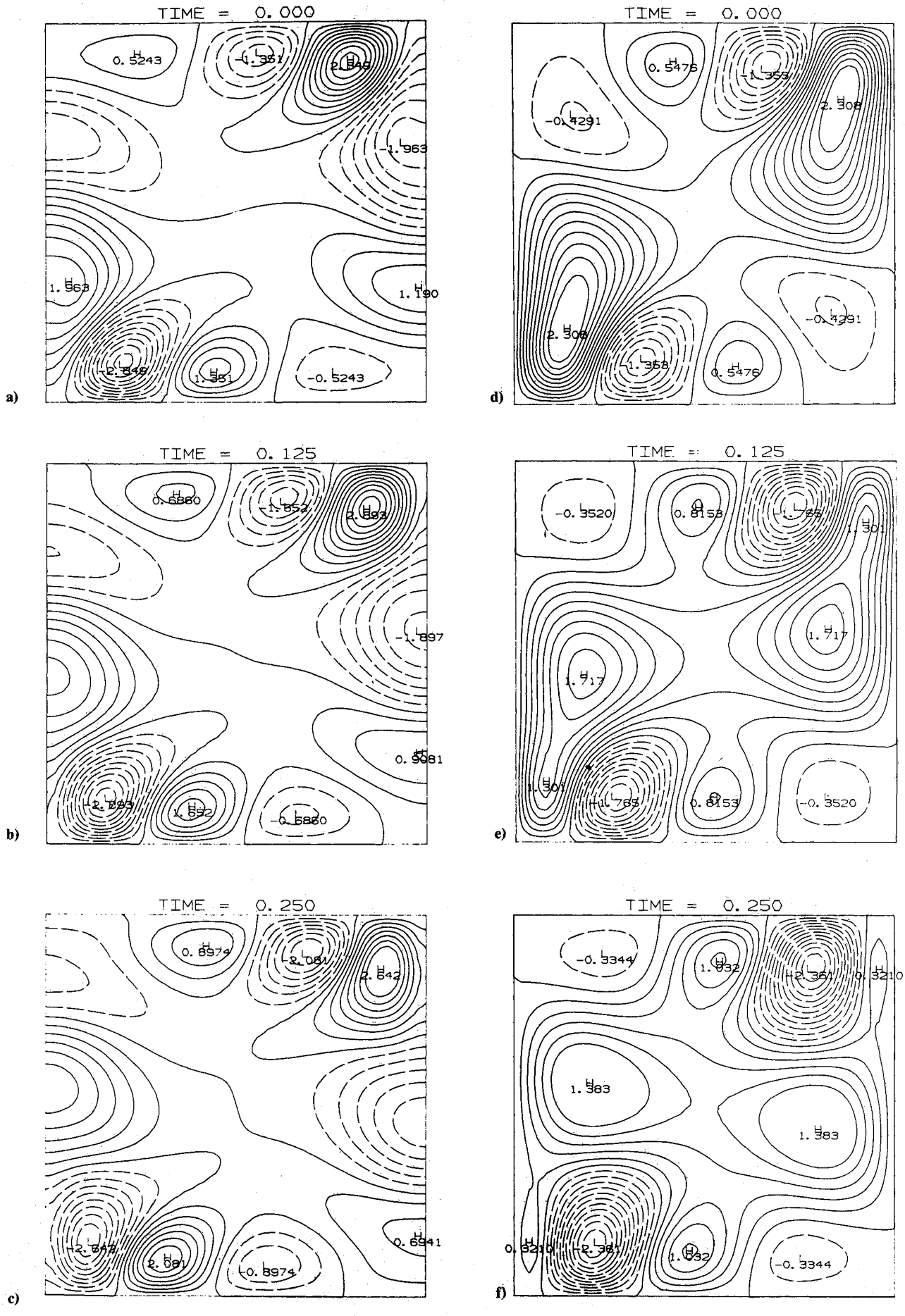

Fig. 3 Unstable disturbances in temperature a)–c) and streamlines d)–f).

functions $i=1$ with wavenumbers $(m,n)=(1,1)$, as described by the linear theory (Ref. 1). There occur $N-1$ subsequent bifurcations occur from the conduction branch, one for each of the remaining modes. Each gives rise to an unstable branch. Hence we focus on the stable branch and follow it in a Rayleigh parameter, using a pseudoarclength continuation technique,[19,20] from its birth up to the transition to time-peridocity. We discuss the effect of the truncation number N on the predicted transition and describe our results, which are obtained by choosing N sufficiently large.

Possible causes of the transition, judged a priori, include a change in the local stability of the branch without loss of existence (e.g., a Hopf bifurcation) or a loss of existence due to a turning point with a resulting change in stability. For an insufficient number of modes, and depending on N, either transition structure can be predicted.

We have systematically increased the maximum wavenumbers considered in our series expansion and find that the predicted value of R_p is sensitive to the maximum wavenumbers considered. Investigators who use spectral or pseudospectral schemes often base the truncation procedure on the criterion that the sum of the wavenumbers remains below a certain level, that is, $m+n\le I$, where I is the order of truncation.[5,8] In contrast, we truncate the terms with individual wavenumbers greater than I, that is, we keep all the terms which satisfy the conditions $m\le I$ and $n\le I$. Our truncation scheme will result in a rectangular rather than triangular form of cutoff and, consequently, additional terms are included in the amplitude equations; however, the advantage of our scheme is that it will conserve the total energy of the system. To see this, note that the net energy transferred between different modes through the nonlinear interactions must balance, since for any (v, Θ) satisfying the boundary conditions of equations (2),

$$\langle \Theta v\cdot \nabla \Theta\rangle = 0 \tag{6}$$

Here the angular brackets indicate integration over the box. Therefore, the term $A_{lmn}a_m a_n$ appearing in the evolution equation for a_l must have counterparts in the evolution equations for a_m and a_n such that

$$A_{lmn}+A_{mln}+A_{nml}=0 \tag{7}$$

In the triangular truncation scheme, when $m+n\le I$ and $l+n>I$, the term $A_{mln}a_l a_n$ will not be considered in the evolution equation for the amplitude a_m. This results in a net addition or subtraction of energy to the system by nonlinear interactions. The overall effect of this inconsistency may be small, however, depending on the physics.

For verification purposes, we will first compare our results with the finite-difference calculation of Caltagirone.[3] Table 1 shows a comparison of the Nusselt number and the value of the maximum stream function at different Rayleigh numbers. Our results presented in Table 1 are obtained with order of truncation $I=18$, and the finite-difference calculations have used a 48×48 mesh system. In all cases the difference between the two results is less than 0.5%.

The predicted value of the critical Rayleigh number for the truncation levels ranging from $I=5$–30 is shown in Table 2. A value of 239 is predicted for order 5, and this value increases with the truncation level until for orders 16, 17, 18, and 30 it converges to the true critical Rayleigh number at $R_p=390.7$. For lower-order truncations we get both a Hopf bifurcation and a turning point as the means of transition to time-periodic motion. For $I=6$, which results in a 21-mode truncation (i.e., $N=21$), a turning point at $R=256$ is obtained. We are unable to obtain a local continuation of steady solutions beyond this point. The results from the eighth-order truncation show the same behavior at $R=304$. For higher-order truncation levels, however, it becomes clear that the transition is due to the loss of the local stability of the steady-state solution or Hopf bifurcation.

The heat transfer across the box, expressed by the Nusselt number

$$Nu\equiv 1-\int_{-1/2}^{1/2}\frac{\partial\Theta}{\partial y}dx = 1-\pi\sum_{n=2}^{I} na_{oon}$$

plotted against the Rayleigh number, is shown in Fig. 1. The frequency of oscillation at the transition point is 82.8 cycles per dimensionless time. This compares favorably with the frequency of 83 cycles per diffusion time at $R_p=389.7$ reported recently.[6]

We now turn to a discussion of the physical mechanism by which the transition takes place. Figures 2a-c and 2d-f show the isotherms and streamlines at Rayleigh numbers 60, 100, and 391, respectively. The flow is rotating clockwise, and it is antisymmetric with respect to the center of the square. Near the convection onset at $R=60$, the flow is uniform. However, the streamlines show that the flow becomes somewhat deformed at higher Rayleigh numbers. The main features of the isotherm plots, resulting from an increase in the Rayleigh number, are the formation of a positive temperature gradient at the core region and the large temperature gradients characterizing the thermal boundary layers at the upper left and lower right corners. The nonlinear amplitude Eqs. (5) are linearized about the finite-amplitude steady state to obtain the pair of linearly independent eigenvectors, that form the two-dimensional subspace in which the Hopf bifurcation resides. Using the components of these eigenvectors, we then calculate the disturbance temperature field and streamlines that become unstable at $R=R_p$. Figures 3a-c and 3d-f show the contour plots of these disturbances at times 0, 1/8, and 1/4 of the oscillation period. The broken lines in these figures represent negative disturbances and the solid lines positive disturbances. The contour plots of the disturbed streamlines show that four pairs of cells, rotating clockwise (solid lines) and counterclockwise (broken lines), have formed inside the container. By comparing the disturbed temperature and streamlines, we see that they are spatially out of phase and that the fluid is rising in the hot regions and descending to the cold regions. It is therefore clear that the disturbed modes that grow are in the form of secondary convection cells that circulate around the container with the main flow. The base-state flow convects the thermal disturbance structure such that at a fixed point in space, the fluid alternatively (in time) moves from warmer to colder thermal disturbances and vice versa in a manner that sustains the oscillation.

In contrast to the behavior at the convection onset where the equations governing the disturbances are self-adjoint, the disturbance equations at R_p are not self-adjoint. The disturbances satisfying the adjoint operator were incorrectly reported by the authors as physical disturbances in a recent conference.[21]

IV. Summary and Conclusions

By means of an eigenfunction expansion method, we follow the unicellular steady-state solution branch using a pseudoarclength continuation technique. Starting from the convection onset at $R_c=4\pi^2$, we trace the solution with various levels of truncation up to the point of transition to time-periodic flow. At lower-order truncations, both the Hopf bifurcation and the turning point are predicted. The predicted critical Rayleigh number increases with the truncation level until it converges to the true value of the critical Rayleigh number at 391. The transition is caused by a Hopf bifurcation.

The isotherms at the point of transition show two features: 1) large temperature gradients forming in the two opposite

corners, and 2) an unstable temperature profile forming at the core region. Therefore, two potential regions of instability are recognized from the characteristics of the main flow. We solve for the disturbed modes that become unstable and show that four pairs of secondary thermal cells have formed and are convected around the container by the main flow. These thermal cells receive their energy indirectly from the thermal boundary layers. The interactions of these cells with the main flow lead the system into a periodic motion.

Acknowledgment

This research is supported by a grant from the Fluid Mechanics program of the National Science Foundation and in part by the U.S. Army Research Office through the Mathematical Sciences Institute of Cornell University. We thank Professor Eusebius Doedel for his assistance in our implementation of his branch-tracing code. Computations were performed on the Cornell National Supercomputer Facility.

References

[1]Beck, J. L., "Convection in a Box of Porous Material Saturated with Fluid," *Physics of Fluids,* Vol. 15, 1972, pp. 1377–1383.

[2]Horne, R. N., "Three-Dimensional Natural Convection in a Confined Porous Medium Heated From Below," *Journal of Fluid Mechanics,* Vol. 92, 1979, pp. 751–766.

[3]Caltagirone, J. P., "Thermoconvective Instability in a Horizontal Porous Layer," *Journal of Fluid Mechanics,* Vol. 72, 1975, 269–287.

[4]Horne, R. N. and O'Sullivan, M. J., "Oscillatory Convection in a Porous Medium Heated From Below," *Journal of Fluid Mechanics,* Vol. 66, 1974, pp. 339–352.

[5]Schubert, G. and Straus, J. M., "Transition in Time-Dependent Thermal Convection in Fluid-Saturated Porous Media," *Journal of Fluid Mechanics,* Vol. 121, 1982, pp. 301–313.

[6]Kimura, S., Schubert, G., and Straus, J. M., "Instabilities of Steady, Periodic and Quasi-Periodic Modes of Convection in Porous Media," *AIAA/ASME 4th Joint Thermophysics and Heat Transfer Conference,* June 2–4, 1986, ASME G00343, HTD-Vol. 56, p. 49.

[7]Combarnous, M. A. and Bories, S. A., "Hydrodynamic Convection in Saturated Porous Media," *Advances in Hydroscience,* Vol. 10, 1975, pp. 270–273.

[8]Kimura, S., Schubert, G., and Straus, J. M., "Route to Chaos in Porous Medium Thermal Convection," *Journal of Fluid Mechanics,* Vol. 166, 1986, pp. 305–324.

[9]Elder, J. W., "Steady Free Convection in a Porous Medium Heated From Below," *Journal of Fluid Mechanics,* Vol. 27, 1967, pp. 29–48.

[10]Schneider, K. J., "Investigation of the Influence of Free Thermal Convection on Heat Transfer Through Granular Material," in *Proceedings of the 11th International Congress of Refrigeration,* Munich, FRG, Paper 11-4, 1963.

[11]Buretta, R. J. and Berman, A. S., "Convective Heat Transfer in Liquid Saturated Porous Layer," *Journal of Applied Mechanics,* Vol. 43, 1976, pp. 249–253.

[12]Combarnous, M. and LeFur, B., "Transfert de Chaleur par Convection Naturelle dans ume Couche Poreuse Horizontale," *Compte Rendus Hebdomadaires des Séances Academie des Sciences,* Paris B, Vol. 269, 1969.

[13]Caltagirone, J. P., Cloupeau, M., and Combarnous, M., "Fluctuating Natural Convection in a Horizontal Porous Layer," in *Compte Rendus Hebdomadaires des Séances Academie des Sciences,* Vol. 273, France, 1971, pp. 833–836.

[14]Caltagirone, J. P., "Fluctuating Natural Convection in Porous Media," *Compte Rendus Hebdomadaires des Séances Academie des Sciences,* Vol. 278, France, 1974, pp. 259–262.

[15]Koster, J. N. and Muller, U., "Free Convection in Vertical Gaps," *Journal of Fluid Mechanics,* Vol. 125, 1982, pp. 429–451.

[16]Koster, J. N. and Muller, U., "Oscillatory Convection in Vertical Slots," *Journal of Fluid Mechanics,* Vol. 139, 1984, pp. 363–390.

[17]Homsy, G. M. and Sherwood, A. E., "Convective Instabilities in Porous Media with Through Flow," *AIChE Journal,* Vol. 22, 1976, p. 168.

[18]Steen, P. H., "Container Geometry and the Transition to Unsteady Benard Convection in Porous Media," *Physics of Fluids,* Vol. 29, 1986, p. 925.

[19]Keller, H. B., "Numerical Solution of Bifurcation and Nonlinear Eigenvalue Problems," *Applications of Bifurcation Theory,* edited by P. H. Rabinowitz, Academic Press, New York, 1977, pp. 359–384.

[20]Doedel, E. J., "AUTO: A Program for the Automatic Bifurcation Analysis of Autonomous Systems," *Congressus Numerantium* 30, 1981, p. 265–284 (*Proceedings of the 10th Manitoba Conference on Numerical Mathematics and Computation,* University of Manitoba, Winnipeg, Canada, 1980).

[21]Aidun, C. K. and Steen, P. H., "Transition to Unsteady Convective Heat Transfer in Fluid-Saturated Porous Medium," AIAA Paper 86-1264, June 1986.